Gluon and gluino penguin diagrams and the charmless decays of the *b* quark

S. A. Abel
Theory Division, CERN CH-1211, Geneva 23, Switzerland

W. N. Cottingham
H. H. Wills Physics Laboratory, Royal Fort, Tyndall Ave., Bristol, BS8 1TL, United Kingdom

I. B. Whittingham
School of Computer Science, Mathematics and Physics, James Cook University, Townsville, Australia, 4811
(Received 20 March 1998; published 1 September 1998)

Gluon mediated exclusive hadronic decays of b quarks are studied within the standard model (SM) and the constrained minimally supersymmetric standard model (MSSM). For all allowed regions of the MSSM parameter space $(A,\tan\beta,m_0,m_{1/2})$ the penguin magnetic dipole form factor F_2^R is dominant over the electric monopole and can be larger than the magnetic dipole form factor of the SM. However, overall the SM electric monopole decay amplitude F_1^L dominates the decay rate. The MSSM penguin contributions to the free quark decay rate approach the 10% level for those regions of parameter space close to the highest allowed values of $\tan\beta$ (~ 55) for which the gluino is light ($m_{\tilde{g}}\approx 360$ GeV) and lies within the range of the six $\tilde{d}$ squark masses. In these regions the supersymmetric box amplitudes are negligible. The MSSM phases change very little over the allowed parameter space and can lead to significant interference with the SM amplitudes. [S0556-2821(98)00919-9]

PACS number(s): 12.15.Ji, 12.60.Jv, 13.25.Hw

I. INTRODUCTION

Supersymmetry (SUSY) is a highly favored candidate theory for new physics beyond the standard model (SM). Of particular interest are the flavor changing neutral current transitions involving the quark-squark-gluino vertex and the non-removable CP-violating phases which arise as the renormalization group equations (RGE) scale the physics down from the unification scale $M_U\sim 10^{16}$ GeV to the electroweak scale. These effects of SUSY have implications for rare B decays and mixings [1–3] and for other observables such as quark electric dipole moments [4,5].

Measurements of rare flavor-changing B decays provide opportunities for the discovery of indirect effects of SUSY [6,7] as the measured observables involve SM and SUSY processes occurring at the same order of perturbation theory. In contrast with the situation for B^0-$\overline{B}^0$ mixing where new physics is expected to change the magnitude of the CP asymmetries but not the patterns of asymmetries predicted by the SM [8], the effects of new physics in decay amplitudes depends on the specific processes and decay channel under consideration and, although small, may be detectable by comparing measurements that within the SM should yield the same quantity.

The $b\to s$ transition provides an opportunity to study CP violation from non-standard phases [9] and there is significant current interest in the $b\to sg$ penguin decay for which it has been argued [10] that enhancement for on-shell gluons is needed from non-SM physics to explain the CLEO measurement [11] of a large branching ratio for $B\to\eta'+X_s$ and the η'-g-g gluon anomaly.

For the gluon-mediated exclusive hadronic decays studied here the effects of SUSY are expected to be small and difficult to disentangle from the SM effects because of the large uncertainties associated with the SM predictions. The SM calculations involve [6] the computation of the quark level decays $b\to qq'\overline{q'}$, the calculation of the Wilson coefficients [12] to incorporate QCD corrections as the physics is renormalized down from the electroweak scale to the scale m_b and, finally, the calculation of hadronic matrix elements for the hadronization of the final-state quarks into particular final states, typically evaluated using the factorization assumption. As this last stage can introduce such large uncertainties that predicted SM rates for exclusive hadronic penguin decays can be in error by a factor of 2 to 3, we will restrict the present study to the weak scale quark level processes where any differences between SM and SUSY physics are more apparent.

The most predictive of the SUSY models is the (constrained) minimally supersymmetric standard model (MSSM) [13,5] based on spontaneously broken $N=1$ supergravity with flat Kähler metrics [14], universal explicit soft-SUSY breaking terms at the scale $M_{\rm MSSM}\sim M_U$ and spontaneous breaking of the $SU(2)\otimes U(1)$ symmetry driven by radiative corrections. Such models contain two CP-violating phases $\delta_{A,B}^{\rm MSSM}$ from the soft-SUSY breaking terms in addition to the usual phase $\delta_{\rm CKM}$ of the Cabibbo-Kobayashi-Maskawa (CKM) mixing matrix. With the usual assumption that these SUSY phases vanish identically at the unification scale because of CP conservation in the SUSY breaking sector, it is claimed [15,6,2,3] that the MSSM predictions for B^0-$\overline{B}^0$ mixing and penguin decays such as $b\to qq'\overline{q'}$ are very similar to those of the SM and that non-minimal SUSY models are needed to obtain any significant non-SM effects. An early study [16] concluded that superpenguin diagrams are small compared to ordinary penguin diagrams unless the

gluino is very light (≈ 1 GeV) and satisfies $m_{\tilde{g}} \ll m_{\tilde{d}}$. Recently Grossman and Worah [8] have found that the gluonic penguin amplitudes for $b \to sq\bar{q}$ and $b \to dq\bar{q}$ in the effective SUSY model of Cohen *et al.* [17] can be up to twice as large as the SM gluonic penguin diagrams and with an unknown phase.

In this paper we revisit the question of MSSM predictions for the penguin mediated decays $b \to qq'\bar{q'}$. In doing so we review in some detail the SM predictions with particular reference to the relative contributions of the internal u, c and t quarks to the gluon penguin diagram [18], the relative magnitudes of the various form factors and the role of the strong and weak phases [19,20]. We find, for example, that the CP violating phases for the $b \to dg$ and $b \to sg$ electric form factors, which dominate the decay amplitude, have no simple relationship with any angle of the unitarity triangle. For the MSSM we explore the allowed regions of the parameter space to locate those regions which give the largest modifications to the SM results. In contrast to the SM, we always find the magnetic amplitude to dominate the electric amplitude. Also, there are large regions of the MSSM parameter space for which the magnetic amplitude is greater than that of the SM. The search for SUSY would be greatly aided if the magnetic amplitudes could be experimentally isolated.

Conservation of the gluonic current requires the $b \to qg$ vertex to have the structure

$$\Gamma^a_\mu(q^2) = \frac{ig_s}{4\pi^2}\bar{u}_q(p_q)T^a V_\mu(q^2)u_b(p_b) \tag{1}$$

where

$$V_\mu(q^2) = (q^2 g_{\mu\nu} - q_\mu q_\nu)\gamma^\nu [F_1^L(q^2)P_L + F_1^R(q^2)P_R] + i\sigma_{\mu\nu}q^\nu [F_2^L(q^2)P_L + F_2^R(q^2)P_R]. \tag{2}$$

Here F_1 and F_2 are the electric (monopole) and magnetic (dipole) form factors, $q = p_b - p_q$ is the gluon momentum, $P_{L(R)} \equiv (1 \mp \gamma_5)/2$ are the chirality projection operators and $T^a (a = 1, \ldots, 8)$ are the $SU(3)_c$ generators normalized to $\mathrm{Tr}(T^a T^b) = \frac{1}{2}\delta^{ab}$.

The $\bar{b} \to \bar{q}g$ vertex is

$$\bar{\Gamma}^a_\mu(q^2) = -\frac{ig_s}{4\pi^2}\bar{v}_b(p_b)T^a \bar{V}_\mu(q^2)v_q(p_q) \tag{3}$$

where $\bar{V}_\mu$ has the form (2) with the form factors $F^{L,R}_{1,2}(q^2)$ replaced by $\bar{F}^{L,R}_{1,2}(q^2)$ where the relationship between the F and $\bar{F}$ form factors will be discussed later.

To lowest order in α_s the penguin amplitude for the decay process $b \to qg \to qq'\bar{q'}$ is

$$M^{\mathrm{Peng}} = -\frac{ig_s^2}{4\pi^2}[\bar{u}_q(p_q)T^a \hat{\gamma}_\mu u_b(p_b)] \times [\bar{u}_{q'}(p_{q'})\gamma^\mu T^a v_{\bar{q}'}(p_{\bar{q}'})] \tag{4}$$

where

$$\hat{\gamma}_\mu \equiv \gamma_\mu [F_1^L(q^2)P_L + F_1^R(q^2)P_R] + \frac{i\sigma_{\mu\nu}q^\nu}{q^2}[F_2^L(q^2)P_L + F_2^R(q^2)P_R]. \tag{5}$$

This gives the free quark decay rate

$$\frac{d\Gamma^{\mathrm{Peng}}}{dq^2} = \frac{1}{288\pi^3}\left(\frac{g_s^2}{4\pi^2}\right)^2 \frac{1}{E_b} I(q^2)\left(1 + \frac{2m_{q'}^2}{q^2}\right)N(q^2) \tag{6}$$

where

$$I(q^2) = \left[1 + \frac{(m_q^2 - q^2)^2}{m_b^4} - 2\frac{m_q^2 + q^2}{m_b^2}\right]^{1/2}\left[1 - \frac{4m_{q'}^2}{q^2}\right]^{1/2} \tag{7}$$

is the phase space factor and

$$\begin{aligned} N(q^2) = {} & (q^2 p_b \cdot p_q + 2p_b \cdot q p_q \cdot q)(|F_1^L|^2 + |F_1^R|^2) \\ & - 3m_b m_q q^2 (F_1^L F_1^{R*} + c.c.) \\ & - 3m_b p_q \cdot q (F_1^L F_2^{R*} + F_1^R F_2^{L*} + c.c.) \\ & + 3m_q p_b \cdot q (F_1^L F_2^{L*} + F_1^R F_2^{R*} + c.c.) \\ & + \frac{1}{q^2}(4p_b \cdot q p_q \cdot q - q^2 p_b \cdot p_q)(|F_2^L|^2 + |F_2^R|^2) \\ & - 3m_b m_q (F_2^L F_2^{R*} + c.c.) \end{aligned} \tag{8}$$

with $4m_{q'}^2 \leq q^2 \leq (m_b - m_q)^2$.

Similarly, for $\bar{b} \to \bar{q}q'\bar{q'}$, the amplitude is

$$\bar{M}^{\mathrm{Peng}} = \frac{ig_s^2}{4\pi^2}[\bar{v}_q(p_q)T^a \bar{\hat{\gamma}}_\mu v_b(p_b)]\bar{u}_{q'}[(p_{q'})\gamma^\mu T^a v_{\bar{q}'}(p_{\bar{q}'})] \tag{9}$$

where $\bar{\hat{\gamma}}_\mu$ is obtained from Eq. (5) by the replacement of all $F(q^2)$ form factors by $\bar{F}(q^2)$ form factors. The decay rate $d\bar{\Gamma}^{\mathrm{Peng}}/dq^2$ is given by Eqs. (6)–(8) with the same replacements.

One CP violation observable of particular interest is the partial rate asymmetry

$$\mathcal{A}_{CP}(q^2) \equiv \frac{d\Gamma_A/dq^2}{d\Gamma_S/dq^2} \tag{10}$$

where

$$\frac{d\Gamma_{S/A}}{dq^2} = \frac{1}{2}\left(\frac{d\Gamma}{dq^2} \pm \frac{d\bar{\Gamma}}{dq^2}\right). \tag{11}$$

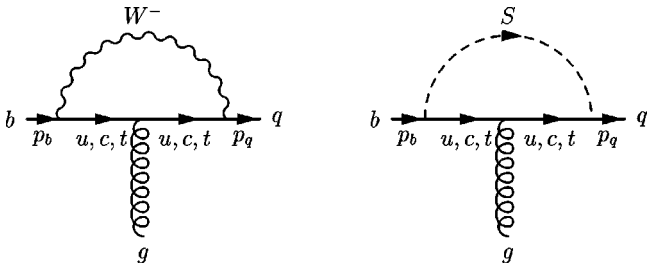

FIG. 1. SM gluon penguins with W and scalar exchange.

II. THE GLUON PENGUIN DIAGRAM IN THE STANDARD MODEL

Although the expressions for the SM form factors are known, we believe it is useful to present a brief outline of their derivation, both in order to clarify their regimes of validity and to aid our later generalization to include the effects of SUSY.

For the SM the contributions to the $b\to qg$ vertex Γ^a_μ from W and scalar exchange (Fig. 1) give [21,22]

$$V^{\rm SM}_\mu(q^2)=\sum_{i=u,c,t}\lambda_i^{bq}[(A^W_\mu+A^S_\mu)P_L+B^S_\mu P_R] \tag{12}$$

where $\lambda_i^{bq}\equiv(g_2^2/8M_W^2)K^*_{iq}K_{ib}$ and K is the CKM matrix. For the $\overline{b}\to\overline{q}g$ vertex $\overline{V}_\mu$, the CKM matrix elements are replaced by their complex conjugates.

After putting the external b and $q(=d,s)$ quarks on mass shell, $V^{\rm SM}_\mu$ has the form

$$V^{\rm SM}_\mu(q^2)=(ap_{b\mu}+bq_\mu+c\gamma_\mu)P_L+(dp_{b\mu}+eq_\mu+f\gamma_\mu)P_R \tag{13}$$

and the form factors for arbitrary q^2 are given by

$$2(m_q^2-m_b^2)F_1^L(q^2)=(a+2b)m_q+(d+2e)m_b \tag{14}$$

$$2(m_q^2-m_b^2)F_1^R(q^2)=(a+2b)m_b+(d+2e)m_q \tag{15}$$

and

$$F_2^L(q^2)=a/2,\quad F_2^R(q^2)=d/2. \tag{16}$$

Neglecting terms of order m_q^2/M_W^2 and m_b^2/M_W^2 then

$$a+2b=-m_q\alpha^{\rm SM},\quad d+2e=m_b\beta^{\rm SM} \tag{17}$$

where

$$\alpha^{\rm SM}(q^2)=\sum_i\lambda_i^{bq}\int_0^1dx\int_0^{1-x}dy[4(x+2y)(y-1)-2x_i(1-x-xy-2y^2)]/Y_i(x,y) \tag{18}$$

$$\beta^{\rm SM}(q^2)=\sum_i\lambda_i^{bq}\int_0^1dx\int_0^{1-x}dy[4x^2-8x+8y^2-8y+12xy+x_i(4x^2-6x+4y^2-8y+10xy+2)]/Y_i(x,y) \tag{19}$$

together with

$$F_2^L(q^2)=m_q\sum_i\lambda_i^{bq}\int_0^1dx\int_0^{1-x}dy[2x(1-y)+x_i(1-x-xy)]/Y_i(x,y) \tag{20}$$

and

$$F_2^R(q^2)=m_b\sum_i\lambda_i^{bq}\int_0^1dx\int_0^{1-x}dy[2x(x+y)+x_i(2x^2-3x+3xy+1)]/Y_i(x,y). \tag{21}$$

In the above

$$Y_i(x,y)=x+x_i(1-x)+q^2[xy+y(y-1)]/M_W^2 \tag{22}$$

where $x_i\equiv m_i^2/M_W^2$.

If these expressions are evaluated at $q^2=0$ we have $\beta^{\rm SM}=\alpha^{\rm SM}$ and

$$F_1^L(0)=\frac{g_2^2}{8M_W^2}\sum_i K^*_{iq}K_{ib}f_1(x_i),\quad F_1^R(0)=0 \tag{23}$$

$$\frac{1}{m_q}F_2^L(0)=\frac{1}{m_b}F_2^R(0)=\frac{g_2^2}{8M_W^2}\sum_i K^*_{iq}K_{ib}f_2(x_i) \tag{24}$$

where [23,24]

$$f_1(x)=\frac{1}{12(1-x)^4}[18x-29x^2+10x^3+x^4-(8-32x+18x^2)\ln x], \tag{25}$$

$$f_2(x)=\frac{-x}{4(1-x)^4}[2+3x-6x^2+x^3+6x\ \ln x]. \tag{26}$$

For small x_i, $f_2(x_i)\approx-\frac{1}{2}x_i$ whereas $f_1(x_i)\approx-\frac{2}{3}\ln x_i$.

For $b\to qg$, $(q^2)_{\rm max}=(m_b-m_q)^2\approx 20\ \ {\rm GeV}^2$ and the assumption $q^2\ll m_i^2$ which would justify the replacement of the form factors with their values at $q^2=0$ is invalid for $F_1(q^2)$ for the u and c quarks. This observation has also been made in [9,18]. For these light quarks we can evaluate $F_1^L(q^2)$ by neglecting m_q^2 compared to m_b^2 in Eq. (14) and x_i in the numerator of Eq. (19) so that

$$f_1(x_i,q^2)=-\int_0^1dx\int_0^{1-x}dy[2x^2-4x+6xy+4y(y-1)]/Y_i(x,y). \tag{27}$$

This integral is dominated by the logarithmic singularity near $x=0$ so we can set $x=0$ everywhere except in the leading term of the denominator to give

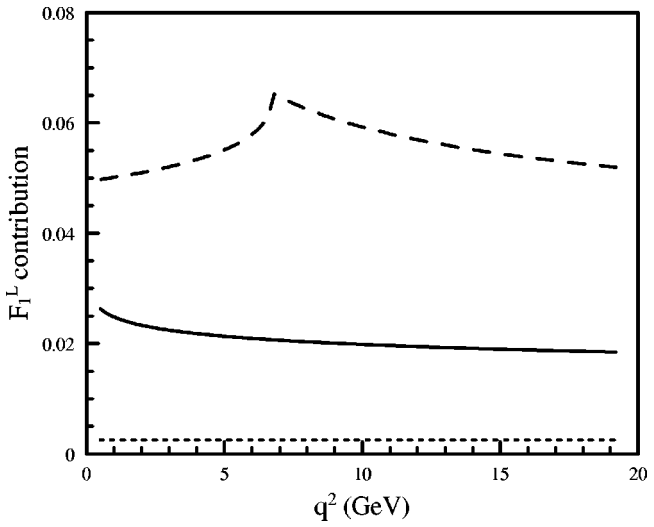

FIG. 2. Contributions to SM $F_1^L(q^2)$ for $b\to d+g$ from u (solid line), c (dashed line) and t (dotted line) quarks.

$$f_1(x_i,q^2)\approx 4\int_0^1 dx\int_0^1 dy\frac{y(1-y)}{x+x_i-q^2y(1-y)/M_W^2} \quad (28)$$

$$=\frac{10}{9}-\frac{2}{3}\ln x_i+\frac{2}{3z_i}-\frac{2}{3}\frac{2z_i+1}{z_i}g(z_i) \quad (29)$$

where $z_i\equiv q^2/4m_i^2$ and

$$g(z)=\begin{cases}\sqrt{\dfrac{1-z}{z}}\arctan\left(\sqrt{\dfrac{z}{1-z}}\right), & z<1,\\ \dfrac{1}{2}\sqrt{\dfrac{z-1}{z}}\left[\ln\left(\dfrac{\sqrt{z}+\sqrt{z-1}}{\sqrt{z}-\sqrt{z-1}}\right)-i\pi\right], & z>1.\end{cases} \quad (30)$$

For $q^2>4m_i^2$, $g(z)$ becomes imaginary due to the generation of a strong phase at the $u\bar{u}$ and $c\bar{c}$ thresholds [19,20]. Our result for $f_1(x_i,q^2)$ is equivalent to that obtained by Gérard and Hou [20]. For the u quark, z_i is large and we use the asymptotic form of Eq. (29):

$$f_1(x_u,q^2)=\frac{10}{9}-\frac{2}{3}\left[\ln\left(\frac{q^2}{M_W^2}\right)-i\pi\right]. \quad (31)$$

We will be concerned with the $b\to dq'\bar{q}'$ and $b\to sq'\bar{q}'$ transitions. Although the form factors F_1 and $(1/m_b)F_2$ contribute to the decay amplitudes (4) and (9) with different kinematic factors, we find that globally over all phase spaces (but with $q^2\geq 1$ GeV^2) the kinematic factors are approximately of equal weight which makes it useful to compare the overall magnitudes of the form factors. We find $F_1^L\gg F_1^R$ and $F_2^R\gg F_2^L$. For the $b\to dq'\bar{q}'$ amplitude we find that F_1^L is dominant $(1/m_b|F_2^R|\lesssim\frac{1}{30}|F_1^L|)$.

The individual contributions $|K_{id}^*K_{ib}f_1(x_i,q^2)|$, $(i=u,c,t)$, to F_1^L are shown in Fig. 2. These magnitudes are

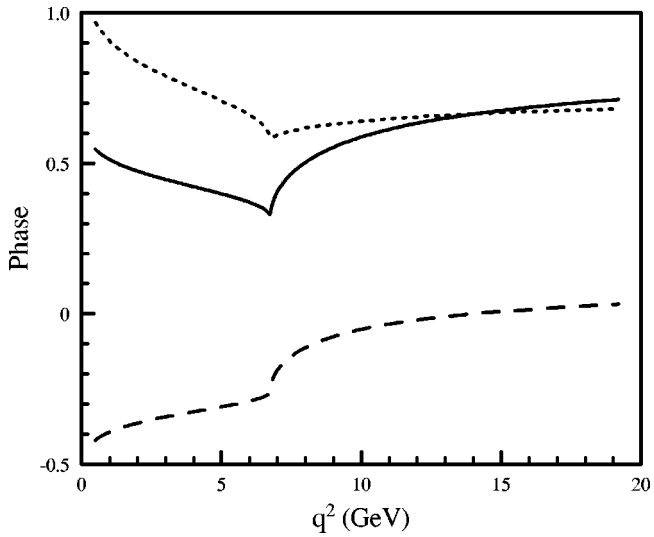

FIG. 3. Phase of SM $F_1^L(q^2)$ for $b\to d+g$ (solid line) and $\bar{b}\to\bar{d}+g$ (dashed line) for a CKM phase of $\pi/2$. The dotted line shows the CP-violating phase difference.

the same for the $\bar{b}\to\bar{d}+g$ transition. The c quark is the largest contributor. The weak phase from the CKM matrix is very small but this contribution carries a strong phase for $q^2>4m_c^2$. This strong phase is the same for the $\bar{b}\to\bar{d}+g$ transition. The u quark contribution has a weak CP-violating phase $e^{-i\delta_{13}}\approx e^{-i\gamma}$ (Particle Data Group notation) and also a strong phase that is common to the $\bar{b}\to\bar{d}+g$ transition. The t quark contribution is negligible.

These individual amplitudes add to make F_1^L and, because u and c make significant contributions, the phase of F_1^L differs for the $b\to d+g$ and $\bar{b}\to\bar{d}+g$ transitions. The phase difference, which can be called the net CP-violating phase, is not negligible but has no simple relationship with any particular angle of the unitary triangle. With $\delta_{13}=\pi/2$ and $s_{13}=0.0035$, we show this phase in Fig. 3.

Because of the presence of both strong and weak phases the magnitudes of F_1^L are also different for the b and $\bar{b}$ decays. Processes like $b\to ds\bar{s}$ and $\bar{b}\to\bar{d}s\bar{s}$ are expected to be penguin dominated and F_1^L dominates all the other form factors. The decay rates $d\Gamma/dq^2$ calculated from Eq. (6) are shown in Fig. 4. The $c\bar{c}$ threshold cusp is clearly exhibited and CP violation is manifest. The difference of the decay rates can easily be shown to be proportional to the Jarlskog factor [25] $\Im[K_{ub}K_{ud}^*K_{cd}K_{cb}^*]=c_{12}c_{13}^2c_{23}s_{12}s_{13}s_{23}\sin\delta_{13}$. Since this factor basically controls the magnitude of the asymmetry, the modification with different choices of s_{13} and δ_{13} (the least known elements of the CKM matrix) can be assessed. The asymmetry is large because the sum of the decay rates is also small.

Turning to the $b\to sq'\bar{q}'$ transition, we again find that $F_1^L\gg F_1^R$, $F_2^R\gg F_2^L$ and the F_1^L amplitude to be dominant. The individual contributions from u, c and t are shown in Fig. 5. The c quark contribution in this case greatly outweighs that of the u and t quarks and since its contribution is so large and has almost zero weak phase, the weak phase on F_1^L is

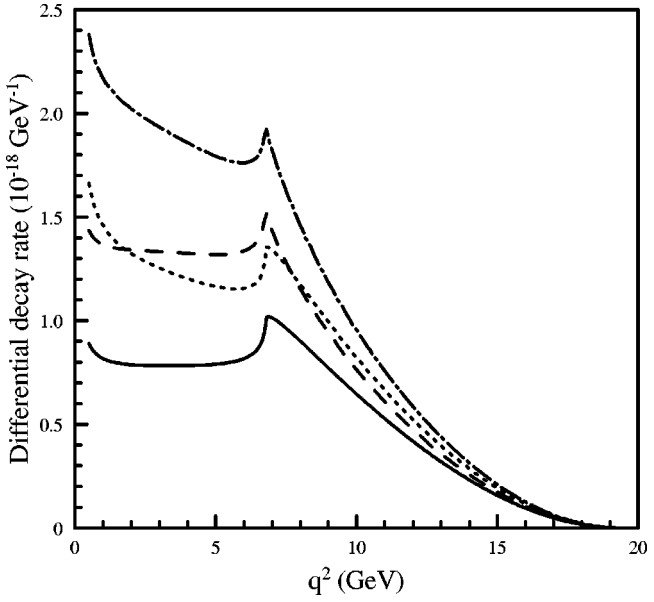

FIG. 4. Differential SM decay rates for $b\to d s\bar{s}$ (solid line) and $\bar{b}\to\bar{d}s\bar{s}$ (dashed line). The corresponding results for the combined effects of the SM and MSSM are given by the dotted and dot-dashed lines respectively.

very small. Processes like $b\to s d\bar{d}$ and $\bar{b}\to\bar{s}d\bar{d}$ are expected to be penguin dominated and these lowest order calculations give the decay rates shown in Fig. 6.

III. THE GLUINO PENGUIN DIAGRAM IN THE MSSM

In the MSSM there are contributions to Γ^a_μ from the two gluino exchange diagrams I and II (Fig. 7) corresponding to the gluon line attached respectively to the gluino and $\tilde{d}$ squark lines. The MSSM penguin amplitudes have the form

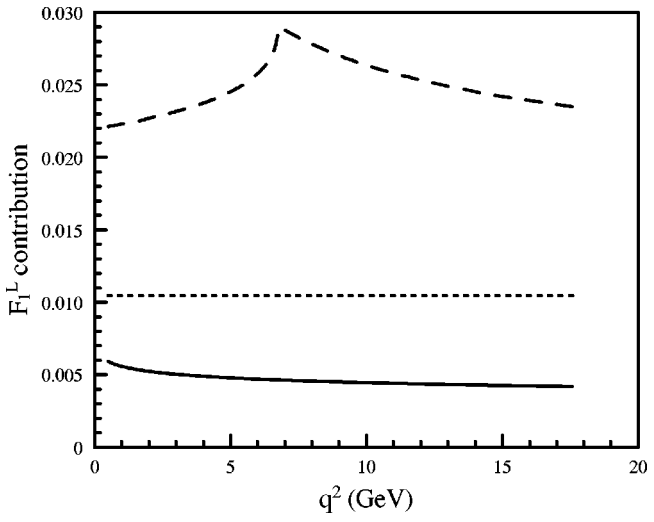

FIG. 5. Contributions to SM $F_1^L(q^2)$ for $b\to s+g$ from u (solid line), c (dashed line) and t (dotted line) quarks. The contribution from the c quark has been scaled down by a factor of 10.

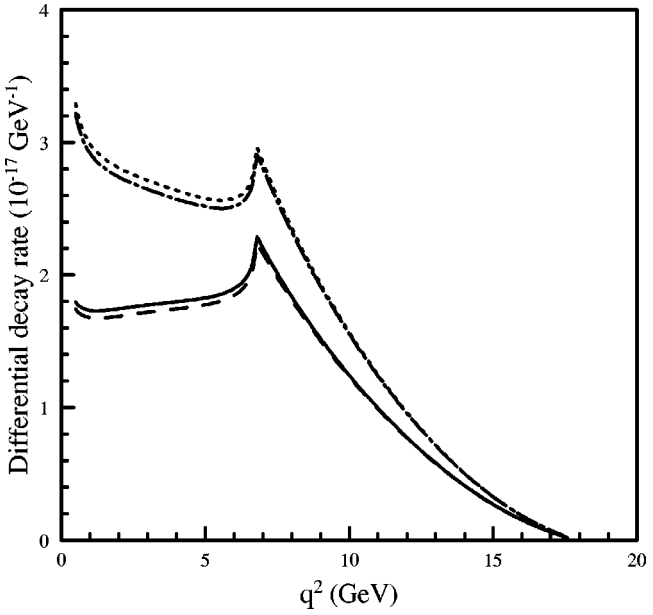

FIG. 6. Differential SM decay rates for $b\to s d\bar{d}$ (solid line) and $\bar{b}\to\bar{s}d\bar{d}$ (dashed line). The corresponding results for the combined effects of the SM and MSSM are given by the dotted and dot-dashed lines respectively.

$$V_{AB}^{\rm MSSM}(q^2)=\sum_j \Lambda^{bq}_{ABj}\{C_2(G)A^{\rm I}_{AB\mu}+[-C_2(G)+2C_2(R)]A^{\rm II}_{AB\mu}\}P_A \tag{32}$$

where (A,B) are chirality indices, $C_2(G)=3$ and $C_2(R)=\Sigma_a T^a T^a=4/3$ are $SU(3)$ Casimir invariants and $j=1,\ldots,6$ labels the d squark mass eigenstates. The coefficient

$$\Lambda^{bq}_{ABj}\equiv -\frac{g_s^2}{4m^2_{\tilde{g}}}V^{jq}_{\tilde{d}B}{}^{*}V^{jb}_{\tilde{d}A} \tag{33}$$

describes the rotation from the down-diagonal interaction states to the $\tilde{d}$ mass eigenstates at the d-$\tilde{d}$-$\tilde{g}$ vertices. The matrices $V_{\tilde{d}L}$ and $V_{\tilde{d}R}$ are obtained from the (6×6) matrix $V_{\tilde{d}}=(V_{\tilde{d}L},V_{\tilde{d}R})^T$ which diagonalizes the $\tilde{d}$ mass^2 matrix

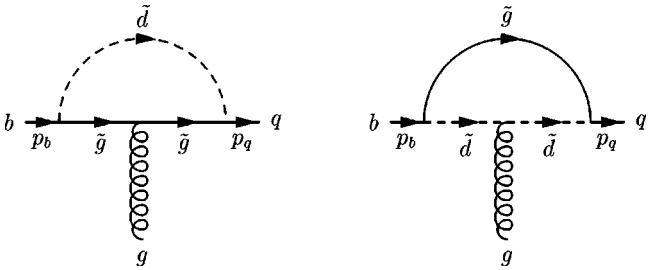

FIG. 7. MSSM gluino penguin diagrams.

$$M^2_{\tilde{d}} = \begin{pmatrix} (M^2_{\tilde{d}})_{LL} & (M^2_{\tilde{d}})_{LR} \\ (M^2_{\tilde{d}})_{RL} & (M^2_{\tilde{d}})_{RR} \end{pmatrix}. \tag{34}$$

Placing the external quarks on mass shell converts $V^{\rm MSSM}_{AB}(q^2)$ into the same general form (13) as for $V^{\rm SM}(q^2)$ so that the MSSM form factors can also be obtained from Eqs. (14)–(16).

For the LL MSSM penguin diagram we find, after neglecting terms of order $m_q^2/m_{\tilde{g}}^2$ and $m_b^2/m_{\tilde{g}}^2$,

$$\alpha^{\rm MSSM}(q^2) = \sum_j \Lambda^{bq}_{LLj} \int_0^1 dx \int_0^{1-x} dy \left\{ C_2(G) \frac{2xy + 4y(y-1)}{Z_j(x,y)} + [-C_2(G) + 2C_2(R)] \frac{2xy - 2y(1-2y)}{Z'_j(x,y)} \right\}, \tag{35}$$

$$\beta^{\rm MSSM}(q^2) = \sum_j \Lambda^{bq}_{LLj} \int_0^1 dx \int_0^{1-x} dy \times \left\{ C_2(G) \frac{2x^2 - 2x + 6xy + 4y(y-1)}{Z_j(x,y)} + [-C_2(G) + 2C_2(R)] \frac{2x^2 - 4x + 6xy + 2(y-1)(2y-1)}{Z'_j(x,y)} \right\} \tag{36}$$

and

$$F_2^L(q^2) = -m_q \sum_j \Lambda^{bq}_{LLj} \int_0^1 dx \int_0^{1-x} dy \left\{ C_2(G) \frac{xy}{Z_j(x,y)} + [-C_2(G) + 2C_2(R)] \frac{xy}{Z'_j(x,y)} \right\}, \tag{37}$$

$$F_2^R(q^2) = m_b \sum_j \Lambda^{bq}_{LLj} \int_0^1 dx \int_0^{1-x} dy \left\{ C_2(G) \frac{x^2 + x(y-1)}{Z_j(x,y)} + [-C_2(G) + 2C_2(R)] \frac{x^2 + x(y-1)}{Z'_j(x,y)} \right\} \tag{38}$$

where

$$Z_j(x,y) = 1 - x + \tilde{x}_j + q^2[xy + y(y-1)]/m_{\tilde{g}}^2, \tag{39}$$

$$Z'_j(x,y) = x + \tilde{x}_j(1-x) + q^2[xy + y(y-1)]/m_{\tilde{g}}^2 \tag{40}$$

with $\tilde{x}_j \equiv m^2_{\tilde{d}_{L_j}}/m^2_{\tilde{g}}$.

As $q^2 \ll m^2_{\tilde{d}_{L_j}}$ we can set $q^2 = 0$ in Eq. (39) and Eq. (40) to get the LL penguin contributions

$$F_1^L(0) = \sum_j \Lambda^{bq}_{LLj} [C_2(G) A(\tilde{x}_j) + C_2(R) B(\tilde{x}_j)], \tag{41}$$

$$F_1^R(0) = 0, \tag{42}$$

$$\frac{1}{m_q} F_2^L(0) = \frac{1}{m_b} F_2^R = \sum_j \Lambda^{bq}_{LLj} [C_2(G) C(\tilde{x}_j) - C_2(R) D(\tilde{x}_j)] \tag{43}$$

where

$$A(x) = \frac{1}{6(1-x)^4} [3 - 9x + 9x^2 - 3x^3 + (1 - 3x^2 + 2x^3) \ln x], \tag{44}$$

$$B(x) = \frac{-1}{18(1-x)^4} [11 - 18x + 9x^2 - 2x^3 + 6 \ln x], \tag{45}$$

$$C(x) = \frac{-1}{4(1-x)^3} [1 - x^2 + 2x \ln x], \tag{46}$$

$$D(x) = \frac{-1}{6(1-x)^4} [2 + 3x - 6x^2 + x^3 + 6x \ln x]. \tag{47}$$

For the LR MSSM penguin diagram

$$\alpha^{\rm MSSM}(q^2) = -\frac{m_{\tilde{g}}}{m_q} \sum_j \Lambda^{bq}_{LRj} \int_0^1 dx \int_0^{1-x} dy \times \left\{ C_2(G) \frac{x + 2y - 1}{Z_j(x,y)} + [-C_2(G) + 2C_2(R)] \frac{x + 2y - 1}{Z'_j(x,y)} \right\} \tag{48}$$

$$\beta^{\rm MSSM}(q^2)=0 \tag{49}$$

and

$$F_2^L(q^2)=m_{\tilde g}\sum_j \Lambda_{LRj}^{bq}\int_0^1 dx\int_0^{1-x} dy\left\{C_2(G)\frac{x-1}{Z_j(x,y)} + [-C_2(G)+2C_2(R)]\frac{x}{Z_j'(x,y)}\right\}, \tag{50}$$

$$F_2^R(q^2)=0. \tag{51}$$

Again we can set $q^2=0$ to obtain for the LR penguin contributions

$$F_1^L(0)=F_1^R(0)=F_2^R(0)=0 \tag{52}$$

and

$$F_2^L(0)=m_{\tilde g}\sum_j \Lambda_{LRj}^{bq}[C_2(G)E(\tilde x_j)-4C_2(R)C(\tilde x_j)] \tag{53}$$

with

$$E(x)=\frac{-1}{(1-x)^2}[1-x+x\ \ln\ x]. \tag{54}$$

The RR and RL penguin diagrams are obtained from the above by the replacements $\Lambda_{LLj}\to\Lambda_{RRj}$ and $\Lambda_{LRj}\to\Lambda_{RLj}$ respectively together with $(-m_q\alpha^{\rm MSSM})\leftrightarrow(m_b\beta^{\rm MSSM})$ and $F^L_{(1,2)}\leftrightarrow F^R_{(1,2)}$.

The total $q^2=0$ MSSM form factors are therefore

$$F_1^L(0)=\sum_j \Lambda_{LLj}^{bq}[C_2(G)A(\tilde x_j)+C_2(R)B(\tilde x_j)], \tag{55}$$

$$F_1^R(0)=\sum_j \Lambda_{RRj}^{bq}[C_2(G)A(\tilde x_j)+C_2(R)B(\tilde x_j)], \tag{56}$$

$$F_2^L(0)=\sum_j \{[m_q\Lambda_{LLj}^{bq}+m_b\Lambda_{RRj}^{bq}][C_2(G)C(\tilde x_j) - C_2(R)D(\tilde x_j)]+m_{\tilde g}\Lambda_{LRj}^{bq}[C_2(G)E(\tilde x_j) - 4C_2(R)C(\tilde x_j)]\}, \tag{57}$$

$$F_2^R(0)=\sum_j \{[m_b\Lambda_{LLj}^{bq}+m_q\Lambda_{RRj}^{bq}][C_2(G)C(\tilde x_j) - C_2(R)D(\tilde x_j)]+m_{\tilde g}\Lambda_{RLj}^{bq}[C_2(G)E(\tilde x_j) - 4C_2(R)C(\tilde x_j)]\}. \tag{58}$$

The results for the $F_2^{(L,R)}(0)$ MSSM form factors agree with those of [26]. However for the $F_1^{(L,R)}(0)$ form factors, whereas our $C_2(R)$ term is the same as that of [26] and [1], the $A(x)$ function occurring in the $C_2(G)$ term differs from that of [26] by $-(1-x)^{-2}\ln x$ and bears little resemblance to the $F(x)$ function of [1]. Note though that our result for $C_2(G)A(x)+C_2(R)B(x)$ is the same as the function $P_F - \frac{1}{9}P_B$ given in [27].

The MSSM calculations are described in [5]. Two-loop MSSM RGEs were used for the gauge and Yukawa couplings and one-loop MSSM RGEs for the other SUSY parameters. Full flavor dependence was included in the running, with one-loop QCD and stop and gluino corrections to the physical top mass from [28]. The unification scale boundary conditions were a universal scalar mass m_0, universal gaugino mass $m_{1/2}$ and a universal soft SUSY-breaking trilinear scalar coupling A. After minimization at the scale m_t of the full one-loop Higgs effective potential, which included all contributions from the matter and gauge sectors, we are left with a four-dimensional parameter space $\{m_0, m_{1/2}, A, \tan\beta\}$, where $\tan\beta\equiv v_2/v_1$ is the ratio of the vacuum expectation values of the two Higgs fields, together with the sign of the coupling μ between the two Higgs fields. The physical Higgs masses were determined using the approximation to the RG-improved Higgs masses described in [29]. Mass eigenvalues and diagonalization matrices for the d squarks were generated for a selection of data sets in the parameter space $150\leqslant m_0\leqslant 1150$; $150\leqslant m_{1/2}\leqslant 1150$; $150\leqslant|A|\leqslant 1150$ (units of GeV) and $2\leqslant\tan\beta\leqslant 48$ which satisfied current experimental constraints (see [30]), and yielded a neutralino as the lightest supersymmetric particle. We also imposed the condition that the standard model like minimum be the global one as has become customary [31]. However it should be noted that, as pointed out in [32], this traditional condition is not *sufficient* to avoid cosmological problems. For this one should employ the slightly more restrictive condition in [32].

The allowed values of A become more restricted by unphysical (charge and color breaking) minima as $\tan\beta$ increases from its fixed point value of $\tan\beta\approx 1.5$ [32]. The avoidance of unphysical minima gives a bound of $m_0/m_{1/2}\gtrsim 1$ at the low fixed point which drops away to about 0.4 at intermediate values of $\tan\beta$. However the minimum bound on $m_0/m_{1/2}$ is for $A\sim m_0$ and it increases quadratically in A away from this value [32], so that effectively $0.5<A<1.5m_0$ at intermediate $\tan\beta$ values. Data sets for negative A were therefore more restricted in this region regardless of the sign of μ, with all but those near m_0 producing color breaking minima. Near the high $\tan\beta$ fixed point, where the bottom Yukawa coupling is large, the analysis of [32] is no longer valid and the parameter space becomes once again less restricted here. Negative and quite large values of A are allowed (and even favored) over positive ones in this region.

Finally we should add that additional and probably very restrictive constraints on m_0 especially at low $\tan\beta$ come from the need to avoid neutralino dark matter overclosing the universe. This was examined recently in [33,34]. However, in order to avoid excluding large regions of parameter space prematurely, this has not been included in the present analysis. Further constraints come from $b\to s\gamma$ (see Ref. [34] and references therein). These processes depend predominantly on the charged Higgs bosons and charginos [when the soft

terms are degenerate at the grand unified theory (GUT) scale] and hence on the value of μ. The resulting constraints can be quite restrictive when $\tan\beta$ is large, with $\mu<0$ being virtually excluded [34,35].

The magnitudes of the MSSM form factors satisfy $|F_2^R|>|F_1^L|\gtrsim|F_2^L|\gg|F_1^R|$ for all regions of the allowed parameter space apart from the narrow region $\tan\beta=2$, $m_{1/2}=150$ and $m_0\gtrsim 1000$ where $|F_1^L|$ is slightly smaller than $|F_2^R|$. Outside this region the ratio $|F_2^R|/|F_1^L|$ exceeds unity and increases strongly with $\tan\beta$. For $\tan\beta=2$, the ratio ranges from ≈ 2 for $m_{1/2}=250$ and $m_0\gtrsim 1000$ to ≈ 9 for low $(m_0,m_{1/2})=(150,250)$. For higher $\tan\beta$, $|F_2^R|$ becomes more dominant, the ratio increasing to 24–28 for $\tan\beta=10$ and 200–225 for $\tan\beta=48$. The relative sizes of the form factors are due to both the mixing coefficients Λ_{ABj}^{bq} (33) and the functions A, B, C, D and E of the variable $\tilde{x}_j\equiv m_{\tilde{d}_j}^2/m_{\tilde{g}}^2$. If the j dependence of $\tilde{x}_j$ is neglected, the quantities $\Lambda_{AB}^{bq}\equiv|\Sigma_j\Lambda_{ABj}^{bq}|$ satisfy $\Lambda_{LL}^{bq}>\Lambda_{RR}^{bq}>\Lambda_{RL}^{bq}>\Lambda_{LR}^{bq}$ and this accounts in the main for the relative sizes of the form factors. The large values of the form factors at high $\tan\beta$ are due to an interplay of two factors: (i) the light gluino mass ($m_{\tilde{g}}\approx 360$ GeV) associated with $m_{1/2}=150$ and (ii) a gluino mass lying within the range of $\tilde{d}$ masses such that the variable $\tilde{x}_j$ is close to unity for several values of j.

The result that F_2^R is the largest MSSM form factor indicates that, in contrast to the SM, the magnetic dipole transition dominates the b decay process in the MSSM. To compare with the SM, we note that the ratio of the largest MSSM and SM form factors is $|F_2^R(\mathrm{MSSM})|/|F_1^L(\mathrm{SM})(q^2=0)|\leqslant 0.4$ GeV.

The phases of the MSSM form factors change very little over the allowed parameter space. The phases of F_1^L and $F_2^{(L,R)}$ are independent of the sign of A and, for $\mu<0$, are approximately equal at ≈ -2.8 for $b\to d$ and ≈ -0.016 for $b\to s$. For $\mu>0$ the phases of $F_2^{(L,R)}$ are shifted by π. The phase of F_1^R varies a little with m_0 and $m_{1/2}$ and depends on the sign of A, being approximately that of F_1^L for $A>0$ and shifted by π from that of F_1^L for $A<0$. These MSSM phases for $\mu<0$ are comparable to the corresponding SM phases so that the magnitude of the phase difference between the dominant MSSM form factor F_2^R and that of the SM form factor $F_1^L(q^2=0)$ is ≈ 0.4 for $b\to d$ and ≈ 0.01 for $b\to s$ for $\mu<0$ and ≈ 2.7 and ≈ 3.1 for $\mu>0$. Hence, after allowance for the negative sign in Eq. (33), we conclude that the super-penguin diagrams and ordinary penguin diagrams have the same sign for $\mu>0$ and opposite sign for $\mu<0$.

IV. SUSY EFFECTS IN $b\to qq'\bar{q}'$

One albeit crude measure of the effects of SUSY in the decays $b\to qq'\bar{q}'$ is the relative size of the integrated decay rates for the MSSM, taken in isolation, and for the SM. In computing these decay rates from Eq. (6) we impose the low q^2 cutoff $q^2\geqslant 1$ GeV to avoid non-perturbative long distance effects.

The largest effects of SUSY on the decay rates occur for high $\tan\beta$ and low $(m_0,m_{1/2})$. For $\tan\beta=48$ and $A=-300$ the ratio $\Gamma^{\mathrm{Peng}}(\mathrm{MSSM})/\Gamma^{\mathrm{Peng}}(\mathrm{SM})$ has a maximum value at $(m_0,m_{1/2})=(275,150)$ of $\approx 0.10(b\to d)$ and $\approx 0.085(b\to s)$ for $\mu>0$ and $\approx 0.09(b\to d)$ and $\approx 0.08(b\to s)$ for $\mu<0$. The ratio exceeds 10^{-2} at $\tan\beta=48$ for $(m_0,m_{1/2})$ ranging from (225,150) to (275,225). However, for lower $\tan\beta$ this ratio has a much smaller maximum value; for $\tan\beta=10$ it is 1×10^{-4} at $(m_0,m_{1/2})=(275,225)$ and 3×10^{-4} at (550,150) for $\tan\beta=2$. The ratio decreases rapidly for large values of $m_{1/2}$ due mainly to the increase of the gluino mass in Eq. (33) from ≈ 360 at $m_{1/2}=150$ to ≈ 1875 at $m_{1/2}=850$. These findings for low and medium $\tan\beta$ differ from the earlier estimates [1] that the SUSY and SM contributions to $\Gamma(b\to sq'\bar{q}')$ were of comparable size. However, these early estimates were based on the assumption that $b\to sq'\bar{q}'$ could be described solely by the LL penguin form factors $F_1^{(L,R)}(0)$ and our study shows F_2^R to be the dominant form factor.

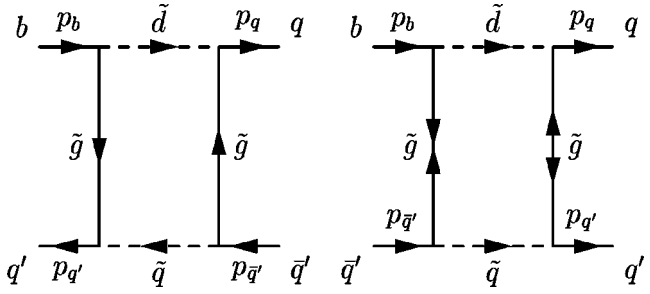

FIG. 8. MSSM box contributions to $b\to qq'\bar{q}'$.

In SUSY there is also a contribution to $b\to qq'\bar{q}'$ from the box diagrams of Fig. 8 for which the amplitude is [1,23]

$$\begin{aligned}M^{\mathrm{Box}}=&\frac{ig_s^2}{4\pi^2}[\bar{u}_q(p_q)T^a\gamma_\mu P_L u_b(p_b)]\\&\times\{J_{LL}^1[\bar{u}_{q'}(p_{q'})\gamma^\mu T^a P_L v_{\bar{q}'}(p_{\bar{q}'})]\\&+J_{LR}^2[\bar{u}_{q'}(p_{q'})\gamma^\mu T^a P_R v_{\bar{q}'}(p_{\bar{q}'})]\}\\&+[\bar{u}_q(p_q)\gamma_\mu P_L u_b(p_b)]\\&\times\{J_{LL}^3[\bar{u}_{q'}(p_{q'})\gamma^\mu P_L v_{\bar{q}'}(p_{\bar{q}'})]\\&+J_{LR}^3[\bar{u}_{q'}(p_{q'})\gamma^\mu P_R v_{\bar{q}'}(p_{\bar{q}'})]\}+(L\leftrightarrow R)\end{aligned}\tag{59}$$

where

$$J_{AB}^\alpha\equiv\sum_{\tilde{d}_j}\sum_{\tilde{q}_i}J_\alpha(\tilde{x}_j,\tilde{y}_i)\Lambda_{AAj}^{bq}V_{qB}^{iq'}{}^*V_{qB}^{q'i}\tag{60}$$

with

$$J_1=\tfrac{7}{6}g(\tilde{x}_j,\tilde{y}_i)-\tfrac{2}{3}f(\tilde{x}_j,\tilde{y}_i),\tag{61}$$

$$J_2=-\tfrac{1}{3}g(\tilde{x}_j,\tilde{y}_i)+\tfrac{7}{3}f(\tilde{x}_j,\tilde{y}_i),\tag{62}$$

$$J_3=\tfrac{2}{9}g(\tilde{x}_j,\tilde{y}_i)+\tfrac{4}{9}f(\tilde{x}_j,\tilde{y}_i).\tag{63}$$

Here $\tilde{y}_i \equiv m^2_{\tilde{q}_i}/m^2_{\tilde{g}}$, the squark $\tilde{q}$ is $\tilde{u}$ for $q'=u$ and $\tilde{d}$ for $q'=d$ and the box functions are [23]

$$g(x,y)=\frac{1}{x-y}\left[\frac{1}{y-1}+\left(\frac{x}{x-1}\right)^2 \ln x-(x\to y)\right] \quad (64)$$

$$f(x,y)=\frac{1}{y-x}\left[\frac{1}{y-1}+\frac{x}{(x-1)^2}\ln x-(x\to y)\right]. \quad (65)$$

For the allowed regions of parameter space the box amplitudes satisfy $|J^2_{LR}|>3(|J^1_{LL}|,|J^3_{LL}|,|J^3_{LR}|) \gg (|J^2_{RL}|,|J^1_{RR}|,|J^3_{RL}|,|J^3_{RR}|)$ apart from in the region $\tan\beta=2$, $m_{1/2}=150$ and $m_0>650$ where $|J^1_{LL}|$ becomes slightly larger than $|J^2_{LR}|$. The four largest box amplitudes are generally of the same order as the MSSM penguin amplitudes $(F^L_1,F^{(L,R)}_2)$; the remaining four are negligible, being smaller by a factor of at least 10^5 and comparable to the MSSM penguin diagram F^R_1. For the regions where $\Gamma^{\rm MSSM}/\Gamma^{\rm SM} \gtrsim 10^{-3}$, the ratio of the largest MSSM box and penguin amplitudes $|J^2_{LR}|/|F^R_2|$ is small, varying from only 8×10^{-3} for the parameters $\tan\beta=48$, $(m_0,m_{1/2})=(275,150)$ which produce the maximum SUSY effects to a maximum of 0.01. The ratio does increase to ≈ 0.4 for low $\tan\beta(=2)$, low $m_{1/2}(=150)$ and high $m_0>1000$ but in these regions the SUSY effects are negligible. Hence, for the MSSM data sets for which the SUSY penguin effects are largest, the SUSY box amplitudes can be neglected in calculating the decay rates.

The differential decay rates $d\Gamma^{\rm Peng}/dq^2$ (6) for the SM and for the combined effects of the SM and the MSSM for the MSSM data set $A=-300$, $\mu>0$, $\tan\beta=48$, $(m_0,m_{1/2})=(275,150)$ which maximizes the SUSY effects show (see Figs. 4 and 6) the SUSY enhancement of the decay rates to be significant for most of the range of q^2 values. The partial rate CP asymmetries $\mathcal{A}_{CP}(q^2)$, defined in Eq. (10), reveal the presence of SUSY for $q^2 \lesssim 4m_c^2$. For these values of q^2 the SM CP asymmetries of $\approx 25\%$ for $b\to d$ and $\approx 1.5\%$ for $b\to s$ are reduced to $\approx 20\%$ and $\approx 1.2\%$ respectively when the MSSM contributions are included.

V. DISCUSSION AND CONCLUSIONS

We have calculated, from first principles, both the SM and MSSM penguin diagrams that contribute to the decays of the b and $\bar{b}$ quarks. For the MSSM in particular there are discrepancies to be found in the literature [26,1] as to the correct formulas for the $F^{(L,R)}_1$ form factors. Our results for these form factors differ slightly from those of [26] but our other results agree with [26].

Because of the presence of strong phases in the contributions to the SM penguin amplitudes from u and c quarks we find that the decay rates for $b\to dq'\bar{q}'$ are significantly different to the rate $\bar{b}\to\bar{d}q'\bar{q}'$ even for quarks in isolation (see Fig. 4).

The SUSY enhancement of the gluon-mediated exclusive hadronic b decays within the constrained MSSM model can be at the several percent level in certain regions of the $(A,\tan\beta,m_0,m_{1/2})$ parameter space. In these regions the SUSY penguin processes dominate the SUSY box processes with the consequence that the b decays in the MSSM are driven by the magnetic dipole transition rather than the electric monopole transition of the SM.

SUSY also introduces penguin processes for $b\to qg$ mediated by charged Higgs bosons, chargino and neutralino exchanges [2]. However, the gluino penguin amplitude is enhanced relative to that for these processes by both the factor α_s/α_W and the additional $\tilde{g}$-$\tilde{g}$-g coupling with its large color factor $C_2(G)=3$ and has been found [2] to be dominant even for much of the low $\tan\beta$ parameter space. Hence the contribution of the charged Higgs boson, chargino and neutralino penguin processes to the decay rate and CP asymmetry should not modify significantly the present results.

QCD corrections arising from renormalization of the present short distance results down from the electroweak scale to the scale m_b are not likely to alter the finding that the magnetic amplitude is dominant in the MSSM as the QCD induced mixing effects [12,36] produce an enhancement of the magnetic dipole operators in the $\Delta B=1$ effective Hamiltonian relative to the current-current penguin operators associated with the electric monopole amplitude. Furthermore, Gérard and Hou [20] have noted that the result (29) for the SM form factor $F^L_1(q^2)$ already contains the dominant part of the QCD corrections for the current-current penguin operators and, therefore, that the main effects of QCD corrections will be the renormalization of the strong coupling constant from $\alpha_s(M_W)$ to $\alpha_s(m_b)$. This would have the effect of increasing the penguin decay rates of the SM by the factor $\eta \equiv \alpha_s(m_b)/\alpha_s(M_W)\approx 1.84$ and also increasing the MSSM penguin amplitudes relative to those of the SM.

Detection of new physics in the hadronic decay amplitudes of the b quark through a study of deviations from the predictions of the SM in the patterns of CP violation in B_d decays is complicated, on the one hand by the interplay between the cumulative effects in the SM of the q^2-dependent strong phases in F^L_1 and the weak CKM phases from the contributing u, c and t quarks and, on the other hand, by MSSM phases comparable in magnitude to the SM weak phases and which can give constructive or destructive interference depending upon the details of the soft SUSY-breaking mechanism.

ACKNOWLEDGMENTS

W. N. Cottingham wishes to thank the PPARC theory travel fund for support for travel to James Cook University.

[1] S. Bertolini, F. Borzumati, and A. Masiero, Nucl. Phys. **B294**, 321 (1987).
[2] S. Bertolini, F. Borzumati, A. Masiero, and G. Ridolfi, Nucl. Phys. **B353**, 591 (1991).
[3] I. I. Bigi and F. Gabbiani, Nucl. Phys. **B352**, 309 (1991); F. Gabbiani, E. Gabrielli, A. Maserio, and L. Silvestrini, *ibid.* **B477**, 321 (1996).
[4] S. Bertolini and V. Vissani, Phys. Lett. B **324**, 164 (1994); T. Inui, Y. Mimura, N. Sakai, and T. Sasaki, Nucl. Phys. **B449**, 49 (1995); T. Falk and K. A. Olive, Phys. Lett. B **375**, 196 (1996); A. Romanino and A. Strumia, Nucl. Phys. **B490**, 3 (1997); M. Aoki, T. Kadoyoshi, A. Sugamoto, and N. Oshimo, hep-ph/9706500; C. Hamzaoui, M. Pospelov, and R. Roiban, Phys. Rev. D **56**, 4295 (1997).
[5] S. A. Abel, W. N. Cottingham, and I. B. Whittingham, Phys. Lett. B **370**, 106 (1996).
[6] M. Gronau and D. London, Phys. Rev. D **55**, 2845 (1997).
[7] J. L. Hewett and J. D. Wells, Phys. Rev. D **55**, 5549 (1997).
[8] Y. Grossman and M. P. Worah, Phys. Lett. B **395**, 241 (1997).
[9] D. Atwood and A. Soni, Phys. Rev. Lett. **79**, 5206 (1997).
[10] W.-S. Hou and B. Tseng, Phys. Rev. Lett. **80**, 434 (1998); A. L. Kagan and A. A. Petrov, hep-ph/9707354.
[11] CLEO Collaboration, P. Kim, talk given at FCNC 97, Santa Monica, California, 1997; CLEO Collaboration, B. Behrens, talk given at Second International Conference on B Physics and *CP* Violation, Honolulu, Hawaii, 1997; J. Smith, talk given at Seventh International Symposium on Heavy Flavour Physics, Santa Barbara, California, 1997.
[12] G. Buchalla, A. J. Buras, and M. E. Lautenbacher, Rev. Mod. Phys. **68**, 1126 (1996).
[13] G. L. Kane, C. Kolda, L. Roszkowski, and J. D. Wells, Phys. Rev. D **49**, 6173 (1994); V. Barger, M. S. Berger, and O. Ohmann, *ibid.* **49**, 4908 (1994).
[14] H.-P. Nilles, Phys. Rep. **110**, 1 (1984); A. B. Lahanas and D. Nanopoulos, *ibid.* **145**, 1 (1987).
[15] M. Ciuchini, E. Franco, G. Martinelli, A. Masiero, and L. Silvestrini, Phys. Rev. Lett. **79**, 978 (1997).
[16] P. Langacker and B. Sathiapalan, Phys. Lett. **144B**, 395 (1984); **144B**, 401 (1984).
[17] A. G. Cohen, D. B. Kaplan, F. Lepeintre, and A. E. Nelson, Phys. Rev. Lett. **78**, 2300 (1997).
[18] R. Fleischer and T. Mannel, Phys. Lett. B **397**, 269 (1997).
[19] M. Bander, G. Silverman, and A. Soni, Phys. Rev. Lett. **43**, 242 (1979).
[20] J.-M. Gérard and W.-S. Hou, Phys. Rev. D **43**, 2909 (1991).
[21] N. G. Deshpande and G. Eilam, Phys. Rev. D **26**, 2463 (1982).
[22] N. G. Deshpande and M. Nazerimonfared, Nucl. Phys. **B213**, 390 (1983).
[23] T. Inami and C. S. Lim, Prog. Theor. Phys. **65**, 297 (1981); **65**, 1772(E) (1981).
[24] W.-S. Hou, Nucl. Phys. **B308**, 561 (1988).
[25] C. Jarlskog, Phys. Rev. Lett. **55**, 1039 (1985).
[26] J.-M. Gérard, W. Grimus, and A. Raychaudhuri, Phys. Lett. **145B**, 400 (1984).
[27] R. Barbieri and A. Strumia, Nucl. Phys. **B508**, 3 (1997).
[28] D. M. Pierce, hep-ph/9407202; J. A. Bagger, K. Matchev, and D. M. Pierce, Phys. Lett. B **348**, 443 (1995); A. Donini, Nucl. Phys. **B467**, 3 (1996); J. A. Bagger, K. Matchev, D. M. Pierce, and R. Zhang, *ibid.* **B491**, 3 (1997).
[29] H. E. Haber, R. Hempfling, and A. H. Hoang, Z. Phys. C **75**, 539 (1997).
[30] P. Janot, talk given at EPS '97 Conference, Jerusalem, 1997, http://www.cern.ch/hep97/talks/t17.ps.gz
[31] J.-M. Frère, D. R. T. Jones, and S. Raby, Nucl. Phys. **B222**, 11 (1983); M. Claudson, L. Hall, and I. Hinchcliffe, *ibid.* **B228**, 501 (1983); H.-P. Nilles, M. Srednicki, and D. Wyler, Phys. Lett. **120B**, 346 (1983); J.-P. Derendinger and C. A. Savoy, Nucl. Phys. **B237**, 307 (1984); J. A. Casas and S. Dimopoulos, Phys. Lett. B **387**, 107 (1996); J. A. Casas, hep-ph/9707475; J. A. Casas, A. Lleyda, and C. Munoz, Nucl. Phys. **B471**, 3 (1996).
[32] S. A. Abel and C. A. Savoy, Report No. CERN-TH-98-64, hep-ph/9803218.
[33] V. Barger and C. Kao, Phys. Rev. D **57**, 3131 (1998); J. Ellis, T. Falk, K. A. Olive, and M. Schmitt, Phys. Lett. B **413**, 355 (1997).
[34] H. Baer, M. Brhlik, D. Castano, and X. Tata, Phys. Rev. D **58**, 015007 (1998).
[35] B. de Carlos and J. A. Casas, Phys. Lett. B **349**, 300 (1995); **351**, 604 (1995).
[36] A. Ali and C. Greub, Phys. Rev. D **57**, 2996 (1998).